Study of the Efficiency and Accuracy of Optimisation Algorithms within Inverse Identification of the Parameter Values of a Nonlinear Concrete Material Model

Petr KRÁL[1], *Jiří KALA*[1], *Petr HRADIL*[1]

[1]Institute of Structural Mechanics, Faculty of Civil Engineering, Brno University of Technology, Veveří 331/95, 602 00 Brno, Czech Republic

kral.p@fce.vutbr.cz, kala.j@fce.vutbr.cz, hradil.p@fce.vutbr.cz

DOI: 10.35181/tces-2019-0013

Abstract. *The inverse identification of the parameter values of nonlinear material models, which have been developed for, inter alia, concrete modelling, is currently a process that is widely used and investigated in the field of research and development. Today there are several approaches that can be employed for the inverse identification process. One of the most significant of these approaches involves the use of optimisation algorithms which, however, often demonstrate varying levels of precision and efficiency within specific tasks. These aspects are the subject of the research presented in this contribution.*

Keywords

Computational model, concrete, experimental data, four-point bend, global optimisation, material model, objective function, optimisation algorithms.

1. Introduction

The modelling of continuum mechanics tasks using nonlinear mechanics tools is currently the main area of focus at many scientific institutions ([1], [2], [3] and [4]). The term "use of nonlinear mechanics tools" refers in particular to the use of geometric and material (physical) nonlinearities within continuum mechanics tasks. The necessity of using geometric or material nonlinearities within numerical calculations is dependent on the type of structure in question and particularly on the selected material from which it will be made. Modern computational systems based on the finite element method ([5], [6], [7] and [8]), which are currently seeing widespread use in the investigation of continuum mechanics tasks, contain a series of methods for the consideration of the nonlinear behaviour of structures, along with many nonlinear material models that can be employed to describe the behaviour of practically any material in the context of numerical simulations. However, the application of nonlinear material models within calculations of a numerical nature gives rise to a fundamental difficulty in terms of the necessity to define the parameters of these models correctly in order for them to function properly. This task often is not very easy as nonlinear material models (and nonlinear material models of concrete in particular) very often include parameters of a purely mathematical nature or parameters which can only be derived using special experimental data. If relevant data which would enable the values of the material model's parameters to be derived directly are not available, the process of the inverse identification of material parameter values can currently be used to deal with this problem ([9], [10], and [11]).

During inverse identification, output data usually consisting of experimental data are generally used to obtain values for material and other parameters. The inverse identification process is therefore based on the combination of experimental data with numerical calculations and identification approaches. The goal is to obtain the best possible approximation of experimental data from numerically simulated data. The most widely used identification approaches today are methods based on the exercise of artificial neural networks [12] and optimisation algorithms [13]. The capability of using optimisation algorithms to perform the inverse identification of parameter values is offered by, e.g. optiSLang software [14], which contains a total of five optimisation algorithms whose efficiency and accuracy can vary for different tasks.

The aim of this paper is to investigate the efficiency and accuracy of optiSLang optimisation algorithms during the inverse identification of values for a small quantity of parameters of the modified version of a nonlinear material model of concrete known as the Continuous Surface Cap Model, which is implemented in the explicit finite element computational system LS-Dyna [15]. For this purpose, a task in the form of a four-point bending test is carried out on a high, steel-reinforced concrete beam. To achieve the set goal, the application of this concrete model and other material models within the computational model of a test created in LS-Dyna is required as well as the use of experimental data obtained from a real four-point bending test. These aspects are described in the following chapters.

2. Material Models

A total of three material models implemented in the LS-Dyna programme were used in the computational model of the four-point bending test. A modified version of the Continuous Surface Cap Model was used to model the behaviour of the high concrete beam. The behaviour of the concrete reinforcement was modelled using the Plastic Kinematic Model and the behaviour of the washers was modelled using the Linear Elastic Model.

2.1. The Continuous Surface Cap Model

The Continuous Surface Cap Model ([16] and [17]) is a nonlinear material model of concrete based on elasto-plastic constitutive theory. The occurrence of plastic deformations is, within the model, controlled by the achievement of a yield surface [18] whose functional relationship can be expressed as:

$$Y(I_1,J_2,J_3)=J_2-\Re(J_3)^2F_f^2(I_1)F_c(I_1,\kappa), \tag{1}$$

where the second member on the right side of the equation is a combination of the shear failure function $F_f(I_1)$ and the hardening model $F_c(I_1,\kappa)$ via a multiplicative formulation. The shear failure function and the hardening model can be expressed mathematically as:

$$F_f(I_1)=\alpha-\lambda\exp^{-\beta I_1}+\theta I_1, \tag{2}$$

$$F_c(I_1,\kappa)=1-\frac{(I_1-L(\kappa))^2}{(X(\kappa)-L(\kappa))^2}\quad\text{for}\quad I_1>L(\kappa), \tag{3}$$

$$F_c(I_1,\kappa)=1\quad\text{for}\quad I_1\le L(\kappa), \tag{4}$$

where:

$$L(\kappa)=\kappa\quad\text{for}\quad\kappa>\kappa_0, \tag{5}$$

$$L(\kappa)=\kappa_0\quad\text{for}\quad\kappa\le\kappa_0, \tag{6}$$

$$X(\kappa)=L(\kappa)+RF_f(I_1). \tag{7}$$

The description of the parameters contained in Eqs. (1)-(7) is as follows: I_1 is the first invariant of the stress tensor, J_2 and J_3 are the second and third invariants of the deviatoric part of the stress tensor, $\Re(J_3)$ is the reduction factor according to Rubin, κ is the hardening parameter, α, β, λ, and θ are material constants which are derived from the experimental testing of concrete in triaxial compression, and R is the ratio parameter of the hardening model.

As the Continuous Surface Cap Model is part of an explicit finite element solver, it enables the effect of the strain rate on the stress state to be considered within its formulation. However, this ability of the model can be neglected during the calculations via the pertinent setting of the model parameter *IRATE* (*IRATE* = 0: calculation with the effect of the strain rate on the stress state → the viscous component of the model is switched off; *IRATE* = 1: calculation with the effect of the strain rate on the stress state → the viscous component of the model is switched on). It can be concluded from the above facts that if the parameter *IRATE* equals zero, the numerically simulated response of the model corresponds to static (slow) loading, which means that it is independent of the velocity of loading used. For this reason, the Continuous Surface Cap Model can be used not only for the numerical modelling of the dynamic loading of concrete structures but also to model the quasi-static or static loading of concrete structures. Within the study described in this paper, the parameter *IRATE* equals zero was used because the static response of the structure was modelled. In order to prevent the dependence of numerical simulation results on the finite element mesh, an algorithm is implemented in the material model which is based on the principle of the crack band model and thus fulfils the function of a localisation limiter.

The modified version of the Continuous Surface Cap Model includes, above and beyond the basic version (25 material parameters), a total of 3 material parameters whose numerical values must be defined. The values of the other parameters are generated automatically based on the values of these three parameters. On the basis of the inverse identification of the values of these three parameters, the efficiency and accuracy of selected optimisation algorithms were tested in this paper. Descriptions and used units are listed for the parameters of the modified version of the Continuous Surface Cap Model in Tab. 1 [15].

Tab.1: Material parameters of the modified version of the Continuous Surface Cap Model.

Parameter	Description of the parameter	Unit
RO	Mass density.	Mg/mm^3
FPC	Unconfined uniaxial compressive strength.	MPa
DAGG	Maximum aggregate size.	mm

2.2. The Plastic Kinematic Model

The Plastic Kinematic Model is a bilinear model based on elasto-plastic constitutive theory. It is suitable for modelling the behaviour of construction steel or steel rebar, or to model the behaviour of plastic material that behaves in a similar manner to steel. The model enables the modelling of a material with hardening, which can be isotropic or kinematic, or without hardening. As the model is part of an explicit finite element solver, it includes the viscous behavioural component. It thus enables, within its formulation, the consideration of the effect of the strain rate on the stress state. However, this ability of the model can be neglected by using zero values for the relevant parameters, as is the case with the Continuous Surface Cap Model.

In calculations carried out for this paper, the viscous component of the model was neglected because the static response of the structure was modelled, and the formulation of the model without hardening was used. The descriptions and units used for the material parameters of the Plastic Kinematic Model, whose values needed to be defined, are listed in Tab. 2 [15].

Tab.2: Material parameters of the Plastic Kinematic Model.

Parameter	Description of the parameter	Unit
RO	Mass density.	Mg/mm^3
E	Young's modulus of elasticity.	MPa
PR	Poisson's ratio.	-
SIGY	Yield strength.	MPa
ETAN	Tangent modulus (*ETAN* = 0: material without hardening).	MPa

2.3. The Linear Elastic Model

As a more detailed material model was not needed for the modelling of the behaviour of the washers, the Linear Elastic Model, or in other words a constitutive model respecting generalised Hooke's Law, was used for this purpose. The descriptions and units used for the material parameters of the Linear Elastic Model, whose values needed to be defined, are listed in Tab. 3 [15].

Tab.3: Material parameters of the Linear Elastic Model.

Parameter	Description of the parameter	Unit
RO	Mass density.	Mg/mm^3
E	Young's modulus of elasticity.	MPa
PR	Poisson's ratio.	-

3. Experimental Data and the Computational Model

3.1. Experimental Data

The experimental data used in this paper are the results of a four-point bending test carried out on a high, steel-reinforced concrete beam. This test was carried out and described within [19]. A schematic representation of the test can be seen in Fig. 1. It shows the geometry of the concrete beam together with the geometry and location of the reinforcing bar and the washers at the points where the loading and support of the beam took place. The material parameters of the hardened (28 days old) concrete and steel rebar were the following, as stated in [19]:

<u>Parameters of the concrete:</u>

- Modulus of elasticity: 20.68 GPa,
- Poisson's ratio: 0.15,
- Uniaxial compressive strength: 24.13 MPa,
- Uniaxial tensile strength: 3.10 MPa.

<u>Parameters of the steel rebar:</u>

- Young's modulus of elasticity: 210.00 GPa,
- Yield strength: 344.75 MPa,
- Cross-sectional area of the reinforcing bar: 0.71×10^{-4} m^2.

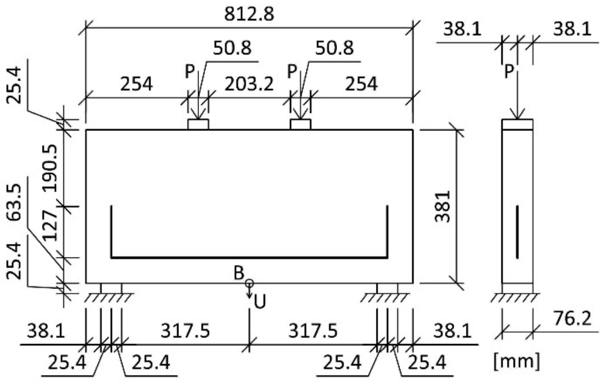

Fig. 1: Schematic representation of the four-point bending test.

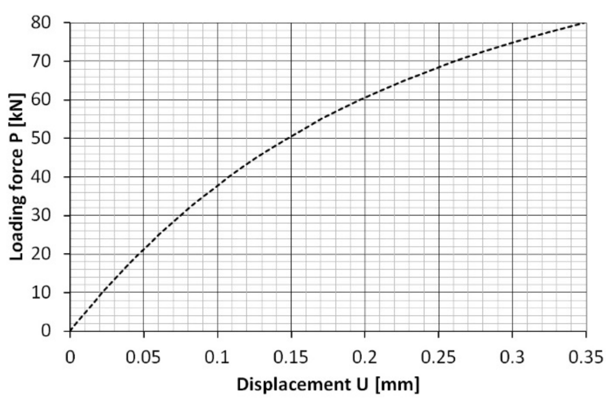

Fig. 2: Measured experimental data.

As shown in Fig. 1, the beam was loaded with forces *P* during the test. The intensity of the forces increased linearly over time until 80 kN was achieved. The velocity of loading was very slow, thus the loading was static. During the test, the vertical displacement (deflection) of beam U was measured at midspan. The exact location where the deflection of the beam was measured is marked with point B in Fig. 1. The measured experimental data are shown in Fig. 2.

3.2. Computational Model

The computational model of the four-point bending test was created in LS-Dyna programme, during which the test scheme from Fig. 1 was respected. The computational model required the creation of finite element models of the high beam, reinforcing bar and washers, and the boundary conditions (supports and loading) had to be defined.

The finite element model of the beam was created using 3D eight-node explicit structural finite elements. The finite element mesh forming the model of the beam was regular (see Fig. 3). As the inverse identification process required the repeated execution of numerical simulations of the task, the symmetry of the task was exploited (only half of the beam was modelled) and the consistence of the finite element mesh of the beam model was chosen in such a way that the time required for the calculation was not too high, which it might otherwise have been due to the use of an explicit finite element algorithm.

The reinforcing bar was modelled using 3D two-node explicit beam finite elements. The consistence of the beam finite element mesh was adapted to the finite element model of the beam in such a way that continuity between the beam and the reinforcing bar model was ensured. The dimensions of the rectangular cross section of the beam finite elements were entered in such a way that the resultant cross-sectional area corresponds to the value from the experiment (0.71×10^{-4} m^2) which is a part of this paper.

The washers were modelled using 3D eight-node explicit structural finite elements. The size of the finite elements forming the models of the washers corresponded to the size of the finite elements forming the model of the beam (see Fig. 3).

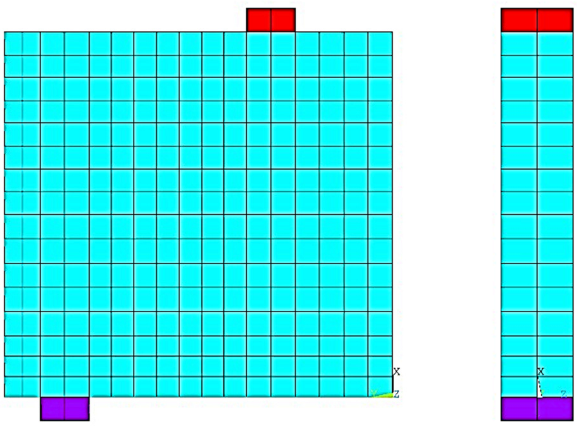

Fig. 3: Finite element model of the investigated task.

The boundary conditions were, within the computational model of the investigated task, defined in the places where washers were located and on the axis of symmetry of the high beam. The model of the bottom washer had its boundary conditions defined in such a way that its displacement was prevented in the horizontal and vertical direction. The model of the top washer had its boundary conditions defined in such a way that its displacement was prevented only in the horizontal direction because of the application of loading. At the location of the axis of symmetry, the symmetric boundary conditions were defined for the model of the beam. Loading was applied to the model of the top washer in the form of pressure linearly increasing over time with a final force of 80 kN. Loading was also applied by considering the structure's self-weight.

4. The Inverse Identification Process

4.1. Global Optimisation and the Optimisation Algorithms Used

For this paper, "global optimisation" was used in order to execute the inverse identification of the values of the parameters of the concrete material model. The aim of global optimisation was to find values for those parameters whose identification were required and whose application would result in numerically simulated data displaying the smallest possible deviation from the experimental data used. This would represent the "reference response" within the inverse identification process. In other words, the global minimum for the selected objective function was sought, along with optimal values for the identified parameters [13]. Global optimisation was carried out using optimisation algorithms in the optiSLang programme, during which their accuracy and efficiency were evaluated. During the optimisation, the selected objective function which characterised the calculation of the Root-Mean-Square Deviation (*RMSD*) was thus minimised. Its mathematical expression was defined by the equation:

$$RMSD = \sqrt{\frac{\sum_{i=1}^{n}\left(U_{calc,i} - U_{ref,i}\right)^2}{n}} \rightarrow \min, \qquad (8)$$

where $U_{calc,i}$ was substituted by numerically simulated vertical displacement (deflection) values corresponding to the pertinent loading force values and $U_{ref,i}$ was substituted by reference (experimentally measured) vertical displacement values corresponding to the same loading force values. Parameter n equalled the number of data defining the resultant shape of the experimental loading curve in Fig. 2 ($n = 32$).

As suggested above, the identified parameters were only parameters of the Continuous Surface Cap Model. The parameters of other material models used were not identified because of their negligible influence on the resultant shape of the numerically simulated loading curve, which was verified by test calculations. The identified parameters formed, within global optimisation, a design vector which can be expressed as:

$$\mathbf{X}_{\mathrm{d}} = \{RO, FPC, DAGG\}^{\mathrm{T}}. \tag{9}$$

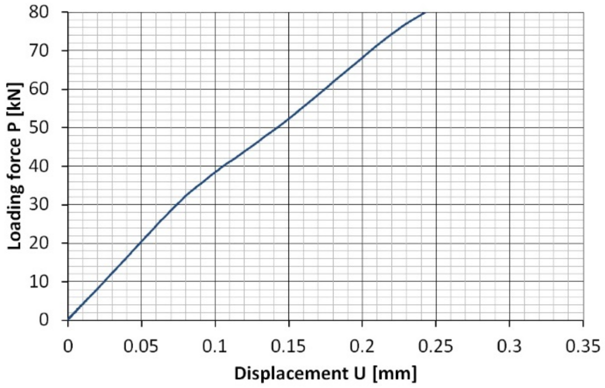

Fig. 4: Numerically simulated data for material parameters from the experiment.

The identified parameters entered the design vector as continuous random variables with a distribution of probability at intervals given by defined boundary values. The limit values of the identified parameters given by the specification of the material model of concrete were used as boundary values [15] (see Tab. 4). Material parameter values from the experiment were used as initial values for the identified parameters, which were necessary for the first generation or iteration of the relevant optimisation algorithm. The numerically simulated loading curve for these parameter values is shown in Fig. 4. Material parameters which were not subject to identification were entered deterministically using values from the experiment (see Tab. 5).

Tab.4: Initial and boundary values of identified parameters.

Parameter	Unit	Initial value	Minimum boundary value	Maximum boundary value
RO	Mg/mm^3	2.400x10^{-9}	2.100x10^{-9}	2.450x10^{-9}
FPC	MPa	24.13000	20.00000	58.00000
DAGG	mm	16.00000	8.00000	32.00000

Tab.5: Parameter values for the material models which were not subject to identification.

Parameter	Unit	Plastic Kinematic Model	Linear Elastic Model
RO	Mg/mm^3	7.850x10^{-9}	7.850x10^{-9}
E	MPa	210000	210000
PR	-	0.3	0.3
SIGY	MPa	344.750	-
ETAN	MPa	0	-

The inverse identification process using optimisation algorithms required the repeated execution of numerical simulations of the investigated task, during which the objective function was minimised. The necessary number of repetitions (or in other words the necessary number of generations or iterations) performed to find the global minimum of the objective function to which the optimal values of the identified material parameters would correspond differed greatly for the different optimisation algorithms (see Tab. 6). For the purposes of this paper a total of five optiSLang optimisation algorithms (briefly described below) were used in order to study their efficiency and accuracy.

Non-Linear Programming by Quadratic Lagrangian (NLPQL)

NLPQL ([14] and [20]) is a sequential algorithm based on nonlinear quadratic programming. This optimisation algorithm is suitable for the solution of tasks which utilise smooth, continuous as well as differentiable objective functions and constraints. The algorithm utilises quadratic approximation of the Lagrangian function and the linearization of constraints.

Simplex Method (Simplex)

The Simplex Method ([14] and [21]) is an iterative optimisation algorithm based on linear programming which is executed systematically with the purpose of determining an optimal solution from a set of feasible solutions. The method is suitable for the optimisation of a low number of parameters.

Adaptive Response Surface Method (ARSM)

ARSM ([14] and [22]) is a direct optimisation algorithm suitable for the optimisation of both low and high numbers of parameters. The main advantage of the algorithm is the fact that it provides an overview of the behaviour of an objective function within the whole design space, it allows the simple inclusion of additional requirements into the objective function, and it also requires a relatively small number of design points.

Evolutionary Algorithm (EA)

The Evolutionary Algorithm ([14] and [23]) is one of a group of optimisation algorithms that utilise processes inspired by biological evolution (i.e. occurring in the natural world), such as mutation, reproduction and recombination. The Evolutionary Algorithm included in optiSLang programme is specifically based on the combination of a genetic algorithm with an evolution strategy.

Particle Swarm Optimisation (PSO)

PSO ([14] and [24]) is one of a group of optimisation algorithms inspired by natural phenomena. To be specific, PSO is a method whose algorithm is inspired by and tries to imitate the behaviour of flocks of birds looking for food.

4.2. Results and Their Evaluation

A table comparison of the results obtained from global optimisation from five different optimisation algorithms is shown in Tab. 6. To be specific, Table 6 shows the resultant optimal values of identified parameters of the modified version of the Continuous Surface Cap Model obtained from the best generations or iterations of the optimisation algorithms, including the relevant minimum values of the objective function which determine the accuracy of the individual optimisation algorithms used. Furthermore, Table 6 also shows the number of iterations or generations of the optimisation algorithms necessary to find the global minimum of the objective function and thus also the optimal values of identified material parameters. These data determine the efficiency of the optimisation algorithms used. Figure 5 shows a graphic comparison of the results, together with the experimental data.

Tab.6: Table comparison of the results.

Parameter	Unit	Optimal value
NLPQL (number of necessary iterations of the algorithm = 21)		
RO	Mg/mm^3	2.400×10^{-9}
FPC	MPa	20.00000
DAGG	mm	8.00000
RMSD	mm	0.0074627
Simplex (number of necessary iterations of the algorithm = 75)		
RO	Mg/mm^3	2.409×10^{-9}
FPC	MPa	20.00000
DAGG	mm	8.00829
RMSD	mm	0.0074597
ARSM (number of necessary iterations of the algorithm = 180)		
RO	Mg/mm^3	2.450×10^{-9}
FPC	MPa	20.00000
DAGG	mm	8.00000
RMSD	mm	0.0074581
EA (number of necessary generations of the algorithm = 400)		
RO	Mg/mm^3	2.450×10^{-9}
FPC	MPa	20.00000
DAGG	mm	28.10027
RMSD	mm	0.0073995
PSO (number of necessary generations of the algorithm = 400)		
RO	Mg/mm^3	2.438×10^{-9}
FPC	MPa	20.00007
DAGG	mm	8.00000
RMSD	mm	0.0074575

The results shown in Tab. 6 and in Fig. 5 show that the accuracy of all of the five optimisation algorithms used was very satisfactory as a very good approximation of the experimental data was achieved by the numerical simulations, during which optimal values were gained for the identified parameters of the material model of concrete used in the individual optimisation algorithms. Moreover, it can be seen that the differences in accuracy between the individual algorithms are practically negligible (the curves practically overlap). However, when looking at the *RMSD* values for the individual algorithms in Tab. 6, it can be concluded that the most accurate optimisation algorithm for the given task is unambiguously the Evolutionary Algorithm (EA).

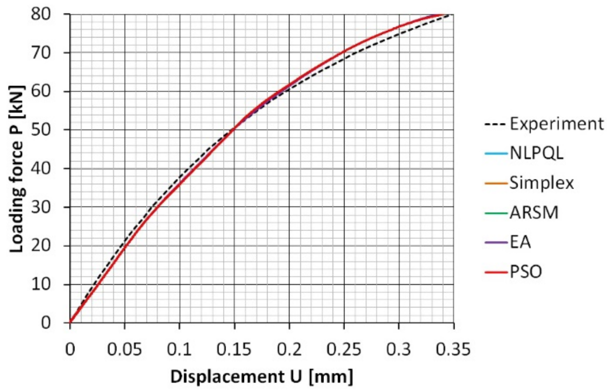

Fig. 5: Graphic comparison of the results.

When looking at Tab. 6 it can additionally be stated that the most efficient algorithm for the given task was clearly the Non-Linear Programming by Quadratic Lagrangian (NLPQL) as this algorithm needed only 21 iterations to find the global minimum of the objective function. It can also be stated that, in contrast, the least efficient optimisation algorithms were the Evolutionary Algorithm and Particle Swarm Optimisation (PSO), as these algorithms needed up to a total of 400 generations to find the global minimum of the objective function.

It can be concluded from the above-mentioned facts that with regard to the accuracy and the finding of the global minimum of the objective function during global optimisation, the Evolutionary Algorithm is the most advantageous, even though this algorithm is not the most efficient with regard to calculation time consumption. Moreover, the optimal value of *DAGG* parameter for the Evolutionary Algorithm differed significantly from the *DAGG* values of other algorithms (see Tab. 6). This difference was due to the existence of two very close minimum peaks of the objective function, of which just one can be classified as the global minimum. Given the smallest *RMSD* value for the Evolutionary Algorithm, it can be concluded that the global minimum of the objective function was just found using this algorithm. In the case of other algorithms, a local minimum which is, however, very close to the global minimum was found. For this reason, the results of all algorithms can be considered as comparable.

Another conclusion is that from the point of view of efficiency, the use of the NLPQL algorithm and possibly also the Simplex Method can be very advantageous for global optimisation as these optimisation algorithms also exhibit very good accuracy, which is comparable with that of the Evolutionary Algorithm.

5. Conclusion

This paper focused on the performing of a study of the efficiency and accuracy of five optimisation algorithms included in optiSLang software during the inverse identification of values for a small number of parameters of the modified version of the Continuous Surface Cap Model implemented in the LS-Dyna computational system. A four-point bending test task was used for this purpose. It was executed on a high, steel-reinforced concrete beam for which a computational model was created, and experimental data were obtained.

The results of the study showed that the accuracy of all five of the optimisation algorithms used was very satisfactory as a very good approximation of experimental data was achieved by the numerical simulations in which the optimal values of identified parameters obtained via the individual optimisation algorithms were used. Moreover, the differences in accuracy between the individual algorithms were practically negligible. However, during global optimisation the most accurate optimisation algorithm was the Evolutionary Algorithm, though it was not the most efficient as far as calculation time consumption is concerned. Also, the results of the study showed that the use of the NLPQL algorithm, and possibly the Simplex Method, can be very advantageous for global optimisation with regard to efficiency. The accuracy of these algorithms was also comparable to that of the Evolutionary Algorithm.

Acknowledgements

This paper was created with financial support of project GACR 17-23578S provided by the Czech Science Foundation and with financial support of the university specific research project FAST-J-18-5604, which was provided by Brno University of Technology.

References

[1] HOKEŠ, F., M. HUŠEK, J. KALA and P. KRÁL. Predicting the Load-Carrying Capacity of Reinforced Concrete Element. *WSEAS Transactions on Applied and Theoretical Mechanics*. 2017, vol. 12, pp. 1–10. ISSN 1991-8749 (print). ISSN 2224-3429 (online).

[2] SUCHARDA, O. and J. BROŽOVSKÝ. Numerical Modelling of Reinforced Concrete Beams with Fracture-Plastic Material. *Frattura ed Integrità Strutturale (Fracture and Structural Integrity)*. 2014, vol. 8, iss. 30, pp. 375–382. ISSN 1971-8993 (online). DOI: 10.3221/IGF-ESIS.30.45.

[3] KRÁL, P., J. KALA and P. HRADIL. Verification of the Elasto-Plastic Behavior of Nonlinear Concrete Material Models. *International Journal of Mechanics*. 2016, vol. 10, pp. 175–181. ISSN 1998-4448 (online).

[4] KRÁLIK, J. Nonlinear Analysis of the Hermetic Postament Safety during Technology Accident in the Nuclear Power Plant. *Transactions of the VŠB – Technical University of Ostrava, Civil Engineering Series*. 2017, vol. 17, iss. 1, pp. 112–121. ISSN 1213-1962 (print). ISSN 1804-4824 (online). DOI: 10.1515/tvsb-2017-0013.

[5] LS-DYNA. Theory Manual. Livemore Software Technology Corporation, Livemore, California, 2018.

[6] ABAQUS. ABAQUS/CAE User's Manual. 2000.

[7] ANSYS. ANSYS Mechanical Theory Reference Release 15.0. 2014.

[8] ADINA. ADINA: Theory and Modeling Guide. *Reports ARD 97-7;97-8*. ADINA R&D Inc. 1997.

[9] HOKEŠ, F., P. KRÁL, M. HUŠEK and J. KALA. Study on Identification of Material Model Parameters from Compact Tension Test on Concrete Specimens. *IOP Conference Series: Materials Science and Engineering*. 2017, vol. 245, pp. 1–10. ISSN 1757-8981 (print). ISSN 1757-899X (online). DOI: 10.1088/1757-899X/245/3/032079.

[10] KRÁL, P., P. HRADIL and J. KALA. Inverse Identification of the Material Parameters of a Nonlinear Concrete Constitutive Model Based on the Triaxial Compression Strength Testing. *Frattura ed Integrità Strutturale (Fracture and Structural Integrity)*. 2017, vol. 11, iss. 39, pp. 38–46. ISSN 1971-8993 (online). DOI: 10.3221/IGF-ESIS.39.05.

[11] HOKEŠ, F., J. KALA and O. KRŇÁVEK. Nonlinear Numerical Simulation of a Fracture Test with Use of Optimization for Identification of Material Parameters. *International Journal of Mechanics*. 2016, vol. 10, pp. 159–166. ISSN 1998-4448 (online).

[12] NOVÁK, D. and D. LEHKÝ. Statistical Material Parameters Identification Based on Artificial Neural Networks for Stochastic Computations. *AIP Conference Proceedings*. 2017, vol. 1858, pp. 1–4. ISSN 0094-243X (print). ISSN 1551-7616 (online). DOI: 10.1063/1.4989942.

[13] MOST, T. Identification of the Parameters of Complex Constitutive Models: Least Squares Minimization vs. Bayesian Updating. In: *Reliability Conference in München*. 2010.

[14] OPTISLANG. Methods for Multi-Disciplinary Optimization and Robustness Analysis. Dynardo GmbH, Weimar, Germany, 2014.

[15] LS-DYNA. Keyword User's Manual. Livemore Software Technology Corporation, Livemore, California, 2018.

[16] MURRAY, Y. D. User's Manual for LS-DYNA

Concrete Material Model 159. *Report No. FHWA-HRT-05-063*. Federal Highway Administration, 2007.

[17] MURRAY, Y. D., A. ABU-ODEH and R. BLIGH. Evaluation of Concrete Material Model 159. *Report No. FHWA-HRT-05-063*. 2006.

[18] SCHWER, L. E. and Y. D. MURRAY. A Three Invariant Smooth Cap Model with Mixed Hardening. *International Journal for Numerical and Analytical Methods in Geomechanics*. 1994, vol. 18, iss. 10, pp. 657–688. ISSN 0363-9061 (print). ISSN 1096-9853 (online). DOI: 10.1002/nag.1610181002.

[19] DAMJANIC, F. and D. R. J. OWEN. Practical Consideration for Modelling of Post-Cracking Concrete Behaviour for Finite Element Analysis of Reinforced Concrete Structures. In: *Proceedings of the International Conference on Computer Aided Analysis and Design of Concrete Structures*. Swansea, U.K.: Pineridge Press, 1984. ISBN 0906674336.

[20] SCHITTKOWSKI, K. NLPQL: A FORTRAN Subroutine Solving Constrained Nonlinear Programming Problems. *Annals of Operations Research*. 1986, vol. 5, iss. 2, pp. 485–500. ISSN 0254-5330 (print). ISSN 1572-9338 (online). DOI: 10.1007/BF02022087.

[21] STONE, R. E. and C. A. TOVEY. The Simplex and Projective Scaling Algorithms as Iteratively Reweighted Least Squares Methods. *Society for Industrial and Applied Mathematics*. 1991, vol. 33, iss. 2, pp. 220–237. ISSN 0036-1399 (print). ISSN 0036-1399 (online). DOI: 10.1137/1033049.

[22] HARDIN, R. H. and N. J. A. SLOANE. A New Approach to the Construction of Optimal Designs. *Journal of Statistical Planning and Inference*. 1993, vol. 37, iss. 3, pp. 339–369. ISSN 0378-3758 (print). ISSN 0378-3758 (online). DOI: 10.1016/0378-3758(93)90112-J.

[23] HRSTKA, O., A. KUČEROVÁ, M. LEPŠ and J. ZEMAN. A Competitive Comparison of Different Types of Evolutionary Algorithms. *Computers & Structures*. 2003, vol. 81, iss. 18–19, pp. 1979–1990. ISSN 0045-7949 (print). ISSN 0045-7949 (online). DOI: 10.1016/S0045-7949(03)00217-7.

[24] KENNEDY, J. and R. EBERHART. Particle Swarm Optimization. In: *Proceedings of IEEE International Conference on Neural Networks*. New York: Institute of Electrical and Electronics Engineers, 1995, pp. 1942–1948. ISBN 0-7803-2768-3. DOI: 10.1109/ICNN.1995.488968.